

# JAAS

Accepted Manuscript



This is an *Accepted Manuscript*, which has been through the Royal Society of Chemistry peer review process and has been accepted for publication.

*Accepted Manuscripts* are published online shortly after acceptance, before technical editing, formatting and proof reading. Using this free service, authors can make their results available to the community, in citable form, before we publish the edited article. We will replace this *Accepted Manuscript* with the edited and formatted *Advance Article* as soon as it is available.

You can find more information about *Accepted Manuscripts* in the [Information for Authors](#).

Please note that technical editing may introduce minor changes to the text and/or graphics, which may alter content. The journal's standard [Terms & Conditions](#) and the [Ethical guidelines](#) still apply. In no event shall the Royal Society of Chemistry be held responsible for any errors or omissions in this *Accepted Manuscript* or any consequences arising from the use of any information it contains.

# Field-Flow Fractionation with Inductively Coupled Plasma Mass Spectrometry: Past, Present, and Future

Pornwilard M-M and Atitaya Siripinyanond\*

Department of Chemistry and Center for Innovation in Chemistry, Faculty of Science, Mahidol University, Rama VI Road, Bangkok 10400, Thailand Fax: +662-354-7151; Tel: +662-201-5195; E-mail: atitaya.sir@mahidol.ac.th

## Abstract

A hyphenated technique of field-flow fractionation (FFF) and inductively coupled plasma mass spectrometry (ICP-MS) is reviewed. The FFF-ICP-MS provides unique information on elemental composition across size or molecular weight distributions. In the early stage of the FFF-ICP-MS development, the technique was found useful for environmental applications. With the growing area of nanotechnology, FFF-ICP-MS has gained increasing interest. A historical background of FFF-ICP-MS is summarized. The key points reported in other previous reviews are summarized. Applications of the FFF-ICP-MS are reviewed to illustrate the potentials of the technique to environmental colloids and nanoparticles. Finally, future prospects of FFF-ICP-MS are considered.

## Introduction

Speaking of the analytical techniques, which provide particle size information, field-flow fractionation (FFF) has been one of major players. Field-flow fractionation is suitable for size fractionation of nanometer and sub-micrometer particles or

1  
2  
3 molecular weight separation of macromolecules of various types, including  
4 environmental particulate materials, suspended clays, aquatic colloids, sediments,  
5 biological cells, viruses, polysaccharides, and others. When the information of size-  
6 based elemental speciation is required, coupling of FFF with atomic spectrometric  
7 techniques, such as ICP-OES and ICP-MS is recommended to offer on-line capability  
8 with high selectivity. Combination of FFF with a sensitive multi-element detector  
9 like ICP-MS allows the determination of the elemental composition across size or  
10 molecular weight distributions [1]. This information about elemental size distribution  
11 is useful for studying processes involving the formation of colloidal-size particulates  
12 and their chemical interactions with associated materials. A specific example is the  
13 study of trace element contaminant transport in waterways [2]. Preferential binding  
14 of specific elements to proteins can be investigated [3].

15  
16  
17  
18  
19  
20  
21  
22  
23  
24  
25  
26  
27  
28  
29  
30  
31  
32  
33  
34  
35  
36  
37  
38  
39  
40  
41  
42  
43  
44  
45  
46  
47  
48  
49  
50  
51  
52  
53  
54  
55  
56  
57  
58  
59  
60

Some differences between FFF and chromatography are based on the types of force used to induce analyte retention. In chromatography, forces are highly selective but at the same time are so powerful that they cause irreversible adsorption and structural disruption, including denaturation. In contrast, the FFF retarding forces are much gentler in nature. For that reason, molecular integrity of macromolecules can be retained during separation. Owing to the absence of solid support in FFF, biological activity loss is minimized compared to chromatography where interaction between analyte molecules and stationary phase is likely to occur. Therefore, FFF is considered a gentle separation technique and can be invaluable in separation of macromolecules especially those with weakly bound or labile species. A schematic diagram representing the FFF separation principle is illustrated in Figure 1.

After a decade of FFF-ICP-MS development in 1991, a summary of FFF hyphenated with ICP was documented in a book chapter published in 2002 [4], which

1  
2  
3 described many features and principles of FFF and highlighted a few examples of  
4 FFF-ICP-MS. By that time, only approximately 19 articles related to the use of FFF  
5 and ICP were reported. Currently, it has been more than two decades since the first  
6 work on FFF-ICP-MS was published. Using the Scopus database from 1991 to  
7 present (May 31, 2014), with the keywords “field-flow fractionation” and  
8 “inductively coupled plasma” searching for the article or review document type, a  
9 total of 119 outputs was found. The publication trend is illustrated in Figure 2. After  
10 the first development of FFF-ICP, the technique grew quite slowly in the first decade,  
11 and a big jump of approximately 400% increase was observed in the last ten years,  
12 suggesting the rapid growth of the technique in the past decade. This might be due to  
13 the blooming area of nanotechnology, where the particle size does matter. This  
14 expands the horizon of the FFF applications from environmental colloids to  
15 nanoparticles (NPs). For the total of 119 articles published, 12 articles are considered  
16 as a review type article, contributing to approximately 10% of the total numbers.  
17 Therefore, the key points in the previous review articles are summarized in this  
18 review.

19  
20  
21 Furthermore, this review describes about the birth and the status of FFF-ICP-  
22 MS in its infancy stage, the use of FFF and ICP in the first decades after the first  
23 report of the technique, selected applications of the technique in the second decade for  
24 inorganic nanoparticles, and environmental colloids. The future trends of the  
25 technique will be forecasted.

### 26 27 28 29 30 31 32 33 34 35 36 37 38 39 40 41 42 43 44 45 46 47 48 49 50 51 52 53 54 55 56 57 58 59 60

**The birth and the early stage of FFF-ICP-MS**

1  
2  
3 In 1991, Beckett introduced the first concepts and described initial experience  
4 in linking FFF separation techniques with ICP-MS [1]. According to Beckett, FFF  
5 yielded accurate and high resolution particle size information for environmental  
6 samples (e.g., suspended colloidal matter from rivers and lakes). Owing to the high  
7 degree of sample dilution taking place during separation in the FFF channel, a very  
8 sensitive analytical technique is needed for subsequent characterization step. In order  
9 to gain morphological, compositional, and adsorption capacity information about  
10 various natural samples, various detection systems, (e.g., optical microscopy,  
11 scanning and transmission electron microscopy, fluorescence, X-ray diffraction,  
12 atomic emission spectrometry, and radioactive tracer techniques), have been used [1].  
13 Until one day, Taylor of the U.S. Geological Survey in Denver suggested that ICP-  
14 MS might be sensitive enough to give elemental information of the fractionated  
15 particles. In addition, ICP-MS could provide multi-element concentration data across  
16 the size distribution of the fractionated sample. With these thoughts, the experiment  
17 on FFF-ICP-MS was then carried out by Beckett, Taylor, and their coworkers [5, 6].  
18 In 1991, the first off-line FFF-ICP-MS experiments were conducted, in which the FFF  
19 separation of suspended matter was carried out in Melbourne (Australia), and the  
20 fractionated components were sent to Denver (USA) for off-line elemental  
21 characterization by using ICP-MS. In the same year, the first on-line experiments  
22 were performed in Denver with the results reported by Taylor et al. in 1992 [5]. In  
23 their work, SdFFF was used to separate three model inorganic solid compounds (i.e.,  
24 lead chromate, aluminum oxide, and iron oxide) suspended in 0.1% tetrasodium  
25 pyrophosphate. Another set of samples was surface-water suspended matter collected  
26 from the Yarra and Darling Rivers in Australia. Major, minor, and trace element  
27 composition of the size-separated colloidal (<1- $\mu\text{m}$  diameter) particulates were  
28  
29  
30  
31  
32  
33  
34  
35  
36  
37  
38  
39  
40  
41  
42  
43  
44  
45  
46  
47  
48  
49  
50  
51  
52  
53  
54  
55  
56  
57  
58  
59  
60

1  
2  
3 measured in the fractionated samples. In addition, Cd adsorption characteristic in the  
4 Yarra River colloid concentrate was studied. Results showed that the amount of Cd  
5 adsorbed per mass of solid adsorbate increased as particle size decreased. The  
6 authors demonstrated that FFF-ICP-MS was an important tool for studying processes  
7 involving the fractionation of colloidal-size particulates and their chemical interaction  
8 with associated materials. To avoid the risk of sample clogging, the Babington-type  
9 pneumatic nebulizer was used to introduce and nebulize suspended particulates into  
10 the ICP torch.  
11  
12  
13  
14  
15  
16  
17  
18  
19  
20  
21  
22  
23  
24

### 25 **FFF-ICP-MS worldwide**

26  
27 Since its introduction in the early 1990s, FFF-ICP-MS has gradually gained  
28 attention. Only approximately 20 publications appeared in the peer-reviewed journals  
29 during the first 10 years after the birth of the technique. The technique grew  
30 relatively slowly as a consequence of the limited number of equipment manufacturers  
31 and their marketing. Only a few FFF manufacturers existed with many distributors  
32 worldwide. These manufacturers include: (1) Postnova Analytics, Munich, Germany  
33 and Postnova Analytics, Salt Lake City, Utah [<http://www.postnova.com>]; (2)  
34 Consensus, Ober-Hilbersheim, Germany [<http://www.consensus.de>]; and (3) Wyatt  
35 Technology Corporation, Santa Barbara, California [<http://www.wyatt.com>]. Another  
36 important reason of why FFF-ICP-MS was of limited use, could be due to the fact that  
37 most ICP-MS users were not trained to be FFF practitioners. Likewise, most FFF  
38 users were not familiar with ICP-MS. Nonetheless, the situation changed when the  
39 nanotechnology began to flourish. Since the FFF-ICP-MS provides great merits and  
40 capabilities to solve important problems, more and more research works on FFF-ICP-  
41  
42  
43  
44  
45  
46  
47  
48  
49  
50  
51  
52  
53  
54  
55  
56  
57  
58  
59  
60

MS have been observed. Collaboration between research groups of different expertise can be helpful.

Publications in the area of FFF with ICP are mostly contributed from the researchers in the USA. Spain, Germany, Australia, ranked number two as a major contributor in publishing the applications of this hyphenated technique, as shown in Figure 3. Considering the contribution from various research groups, Colorado School of Mines ranked number one, followed by Monash University as number two, and University of Gothenburg together with Mahidol University as number three (Figure 4). Both oral and poster presentations related to the use of FFF and ICP have been made at many major conferences in the atomic spectroscopic community, including the 2013 European Winter Conference on Plasma Spectrochemistry in Krakow, Poland, and the 2014 Winter Conference on Plasma Spectrochemistry in Amelia Island, Florida, USA.

To summarize the key points related to FFF with ICP-MS detection in the other review articles, the selected contents in those review articles are highlighted in the following section. Then, some selected recent applications of the technique for environmental colloids and engineered nanoparticles are discussed.

### **Review articles related to FFF-ICP-MS**

Various review articles related to the use of FFF and ICP for several investigations were reported. However, the tutorial review, which is directly devoted to FFF and ICP-MS coupling, was reported in 2010 by Dubascoux et al. [7]. This review emphasizes on some key elements regarding the interface between FFF and ICP-MS including the history and practical aspects, and also described about the

1  
2  
3 applications of the technique for qualitative and quantitative analyses. The interface  
4 between FFF and ICP-MS can be a simple connection through a PEEK (polyether  
5 ether ketone) or PFA (perfluoroalkoxy alkane) tube between the outlet of FFF system  
6 and the sample nebulizer of the ICP-MS system when the flow rate outlets are  
7 compatible with the ICP-MS nebulizer. If not, a split connection might be used when  
8 the flow rate outlets were too high. The important thing to consider is the issue of  
9 particle size selectivity in the nebulizer-spray chamber system. Regarding the  
10 applications of the technique, the authors stated that more than 90% of papers were  
11 contributed to environmental applications, but only a few papers enlarged the  
12 application field with industrial applications, food sciences, and life sciences. The  
13 authors summarized some selected applications of FFF-ICP-MS in various  
14 applications including environmental, bioapplications, nanoparticles, and others. The  
15 feature of flow FFF to allow sample preconcentration was also mentioned to cope  
16 with high dilution associated with the inherent principle of the fractionation during  
17 FFF analysis.

18  
19  
20  
21  
22  
23  
24  
25  
26  
27  
28  
29  
30  
31  
32  
33  
34  
35  
36  
37  
38  
39  
40  
41  
42  
43  
44  
45  
46  
47  
48  
49  
50  
51  
52  
53  
54  
55  
56  
57  
58  
59  
60

The other review articles related to FFF with ICP-MS are not directly devoted to this hyphenated technique. However, FFF with ICP-MS was listed together with other techniques for certain applications. The reviews were focused either on engineered nanoparticles or environmental colloids.

For the engineered nanoparticles, various review articles were published [8-10]. The review by Tiede et al. [8] discussed about different analytical techniques available for the detection as well as physical and chemical characterization of engineered nanoparticles in product formulations, environmental matrices and food materials. The authors emphasized the importance of the physical and chemical properties of the engineered nanoparticles within the sample and the chemical

1  
2  
3 characteristics of any capping/ functional layer on the particle surface. The analytical  
4  
5 techniques should be sensitive enough to measure low concentrations, and also  
6  
7 minimize sample disturbance. This review categorized a range of analytical  
8  
9 techniques into various approaches including microscopy, chromatography,  
10  
11 centrifugation and filtration, and spectroscopic techniques, and related techniques.  
12  
13 Field-flow fractionation was listed as one of chromatographic related techniques  
14  
15 which can provide information on particle number concentration, shape, and size.  
16  
17 The FFF technique was discussed as a highly promising technique for size separation  
18  
19 of ENPs in complex natural samples. Despite the fact that it is a mild and versatile  
20  
21 fractionation technique, careful optimization of carrier composition demands  
22  
23 experience and attention should be paid to minimize the membrane interactions.  
24  
25 Coupling FFF with ICP-MS is not only possible to quantify different nanoparticles in  
26  
27 food, water, biota and soil, but also to characterize or elementally analyze them.  
28  
29  
30

31  
32 Jiménez et al. [9] described the use of several separation techniques with ICP-  
33  
34 MS detection to the analysis of natural and engineered nanoparticles in the  
35  
36 environment. They categorized the review into different parts as follows: natural  
37  
38 nanoparticles analysis by polyacrylamide gel electrophoresis laser ablation ICP-mass  
39  
40 spectrometry (PAGE-LA-ICP-MS); engineered nanoparticle analysis by separation  
41  
42 techniques coupled to ICP-MS; and identification and characterization of engineered  
43  
44 nanoparticle by single particle detection. To hyphenate with ICP-MS detection, FFF  
45  
46 was described as one of separation techniques used for separation, apart from size  
47  
48 exclusion chromatography, and hydrodynamic chromatography.  
49  
50

51  
52 A critical review on the application of plasma spectrometry for the analysis of  
53  
54 engineered nanoparticles was given by Krystek et al. [10]. This review covers the use  
55  
56 of ICP technique for the determination of ENPs and when applied in various  
57  
58  
59  
60

1  
2  
3 consumer's products including possible release during use. The authors stated the  
4 importance of sample handling and sample preparation for analysis with plasma  
5 spectrometry. Care must be taken to preserve size stability. Among all the  
6 hyphenated techniques for the analysis of ENPs, FFF coupled with ICP-OES or ICP-  
7 MS was also described in the review as a size fractionation technique for the cases of  
8 complex mixtures of NPs. With FFF, questions related to membrane-nanoparticle  
9 interaction, behaviors of different nanoparticle types in the FFF channel, and the  
10 influence of dilution of suspensions during separation should be considered. Also,  
11 development of the suitable calibration strategies or the improvement of recovery  
12 should be carried out.

13  
14  
15  
16  
17  
18  
19  
20  
21  
22  
23  
24  
25 Fedotov et al. [11] reviewed the techniques for fractionation and  
26 characterization of nanoparticles and microparticles in liquid media. Among all other  
27 techniques, FFF was listed as one versatile technique for such purpose. Three modes  
28 of FFF separation were mentioned including normal, steric, and hyperlayer. Various  
29 sub-techniques of FFF were described. The authors mentioned that the homogeneous  
30 samples should be used to obtain representative data, as in FFF the sample weight is  
31 less than 1 mg. Additionally, with a very small sample weight, the detection  
32 techniques for the analysis of the separated fractions should be highly sensitive.  
33 Applications of asymmetrical flow FFF (AF4) coupled online with ICP-MS for study  
34 metal associations to different environmental microparticles, nanocolloids, and  
35 macromolecules were mentioned.

36  
37  
38  
39  
40  
41  
42  
43  
44  
45  
46  
47  
48  
49  
50 The applications of flow FFF (FIFFF) for the characterization of natural  
51 colloids and natural and manufactured nanoparticles with the emphasis on the  
52 detection systems were reviewed by Baalousha et al. [12]. Various detection  
53 techniques were mentioned including UV-Vis, organic carbon detector, fluorescence,  
54  
55  
56  
57  
58  
59  
60

1  
2  
3 ICP-MS and ICP-OES, laser-induced breakdown detection, multi angle light  
4 scattering, dynamic light scattering, transmission electron microscopy, and atomic  
5 force microscopy. With FIFFF, calculation of the hydrodynamic diameter is based on  
6 applying Stokes' relationship assuming that particles are hard spheres. However, not  
7 all the cases that the particles are spherical in shape, suggesting the need for a detector  
8 giving an independent and complimentary measurement of the particle size  
9 distribution. The authors discussed about the use of multi detection approach to help  
10 verifying any abnormalities and deviation from theoretical principles of the  
11 fractionation, and in some cases to help providing a wide range of information on  
12 other particle properties such as composition, concentration, optical properties,  
13 interaction with trace metals, and structure. In their review, the operational conditions  
14 of FIFFF and the study objective for the analysis of natural colloids and natural  
15 nanoparticles were summarized. The natural colloids include extracted humic  
16 substances, river and lake waters, estuaries and marine water, wastewater, soil,  
17 sediment, and groundwater, atmospheric particles. For the manufactured  
18 nanoparticles, measurements of the thickness of surface coating, structure and  
19 aggregation behavior were discussed.

20  
21  
22  
23  
24  
25  
26  
27  
28  
29  
30  
31  
32  
33  
34  
35  
36  
37  
38  
39  
40  
41 The review by Lespes and Gigault [13] also discussed about the use of  
42 different hyphenated techniques to obtain multidimensional information for  
43 characterization of submicron particles. Hyphenation of an on-line fractionation to  
44 one or several complementary detectors was illustrated to be useful. Field-flow  
45 fractionation was listed as one of the techniques, which could provide separation  
46 before the detection. In comparison with other techniques, the FFF offered  
47 advantages in the sense that fractionation power and dynamic range could be easily  
48 tuned by varying the field strength. Various sub-techniques of FFF were mentioned.  
49  
50  
51  
52  
53  
54  
55  
56  
57  
58  
59  
60

1  
2  
3 Detection was classified into the category that could provide particle concentration,  
4 particle size, elemental concentration, molecular structure information, and other  
5 more specific information. When the information on elemental concentration is  
6 sought, inductively coupled plasma spectroscopy was listed as a technique of choice.  
7  
8 Various techniques were discussed and compared for their advantages and limitations.  
9  
10

11  
12 For environmental samples, Contado et al. [14] discussed about different  
13 methodologies to fractionate and characterize riverine suspended particulate matter.  
14 The review also described about various experimental approaches to perform  
15 sampling and preconcentration. These included membrane filtration, tangential flow  
16 filtration, centrifugation, and continuous flow centrifugation. For size fractionation,  
17 sequential continuous flow centrifugation, tangential flow filtration, split-flow thin-  
18 channel fractionation (SPLITT), and FFF were mentioned. Among these techniques,  
19 FFF and SPLITT preserved the complexity of the colloidal feature and useful for  
20 quantitative approaches to study trace metal distribution on suspended particulate  
21 matter, particularly when element specific detectors as GFAAS or ICP-MS were used.  
22  
23  
24  
25  
26  
27  
28  
29  
30  
31  
32  
33  
34  
35

36 Another review described the various components of FIFFF instrumentation,  
37 the nature of the separation process and the theory for translating retention time to  
38 relative molecular mass [15]. This review focused on the symmetrical FIFFF  
39 subtechnique. The use of frit inlet and outlet feature was described. The frit inlet  
40 offers rapid hydrodynamic relaxation of the sample components to reach their  
41 equilibrium positions without having to stop the channel flow, thereby avoiding  
42 disruption in the channel. The frit outlet was used for skimming off the carrier liquid  
43 through the frit materials and thereby allowing the concentrated particles to flow to  
44 the detection system, and therefore the detection sensitivity was increased. Regarding  
45 the carrier liquid, not only that the ionic strength and the effective dispersion of the  
46  
47  
48  
49  
50  
51  
52  
53  
54  
55  
56  
57  
58  
59  
60

1  
2  
3 particles need to be considered, it should also be properly chosen to minimize  
4 swelling of the membrane, which could lead to non-uniform flows in the channel.  
5  
6 Also, care must be taken to avoid potential interference with detector response,  
7 interactions with channel materials. Detectors should be selected according to  
8 information seek for the sample being analyzed. Two operating modes, including  
9 normal and steric/hyperlayer modes were discussed. The applications of FIFFF to  
10 environmental and biological matrices and the detection of polymers and inorganic  
11 colloids were summarized by listing the analytes, the membrane, the carrier, and the  
12 detector used. The authors commented that in order to establish a broader user base  
13 with appropriate practical support, the publication of “standard” analytical methods  
14 for particular applications might be needed.  
15  
16  
17  
18  
19  
20  
21  
22  
23  
24  
25  
26

27  
28 The review by von der Kammer et al. [16] presented the current status of FFF  
29 as an analytical separation technique for the study of NPs in complex food and  
30 environmental samples. The ability to identify the ENPs among the background of all  
31 other NPs in the sample is quite challenging. With this, the development of a proper  
32 sample-preparation procedure or the use of element specific detector may be  
33 considered. Sample preparation should be carried out in such a way that a stable  
34 suspension of particles is obtained. The authors commented on different approaches  
35 to separate NPs from a certain matrix, such as particle settling, centrifugation, or  
36 filtration. Using settling and centrifugation minimized the risks of sample alterations,  
37 whereas the membrane filter cannot guarantee that particles smaller than the  
38 membrane cut-off indeed pass the membrane quantitatively. For natural NPs which  
39 are generally complex, heterogeneous, and present as broad size range, careful  
40 optimization of the FFF operating conditions must be carried out in order to obtain the  
41 full range of sizing. In addition, optimization must be carried out to separate the  
42  
43  
44  
45  
46  
47  
48  
49  
50  
51  
52  
53  
54  
55  
56  
57  
58  
59  
60

1  
2  
3 analytical part of the fractogram completely from the void peak, and the mixed modes  
4 of elution (normal and steric mode) should be avoided. In general, the carrier liquid  
5 should prevent particle dissolution and aggregation. Normally, the carrier liquid  
6 should provide sufficient electrostatic repulsion to prevent attachment and loss of the  
7 particles to the membrane. The membrane should be chosen to provide enough  
8 repulsion between the particles and the membrane surface, but not too high to cause a  
9 repulsion-cushion effect causing the early elution of the particles. For the detection,  
10 FFF may be coupled with many types of detectors. When the ICP-MS is used, the  
11 particle size dependent nebulization and ionization efficiencies in the ICP should be  
12 concerned.  
13  
14  
15  
16  
17  
18  
19  
20  
21  
22  
23  
24  
25  
26  
27  
28  
29

### 30 **Selected applications of FFF-ICP-MS**

31  
32 Considering the applications of FFF-ICP-MS, most of the publications are  
33 related to environmental colloids and inorganic nanoparticles. Therefore, some recent  
34 applications of the technique are reviewed in the following sections.  
35  
36  
37  
38  
39  
40

#### 41 **Environmental colloids**

42  
43 With FFF-ICP-MS, size-based elemental speciation can be performed. The  
44 information on elemental concentration across size distribution information is  
45 obtained. FFF-ICP-MS also allows the detection of specific binding of elements to  
46 various nanocolloids sub-fractions. This information can be important and useful to  
47 gain insight into metal transport and fate. Brief findings of FFF-ICP-MS experiments  
48 on environmental applications are summarized as follows:  
49  
50  
51  
52  
53  
54  
55  
56  
57  
58  
59  
60

1  
2  
3 Bolea and Castillo [17] established the methodology based on asymmetrical  
4 flow field-flow fractionation (AF4) coupled with ICP-MS to characterize metal  
5 association to environmental particles of a wide range sizes from 1 kDa to 50  $\mu\text{m}$ . In  
6 AF4, both steric (microparticle) and normal (nanocolloids and macromolecules)  
7 modes of AF4 were performed with prefractionation steps, sedimentation, and  
8 centrifugation. Four crossflow programs were used to classify environmental  
9 particles into four groups as microparticles eluted in the steric mode ( $> 1 \mu\text{m}$ ),  
10 nanocolloids eluted in the normal mode (15 nm to 1  $\mu\text{m}$ ), macromolecules up to 1,000  
11 kDa, and macromolecules less than 100 kDa. To correct for ICP-MS instrumental  
12 drift, Cs internal standard solution was mixed with the outlet stream of AF4. Al and  
13 Si were mainly found as the microparticles, with which Zn and Pb were significantly  
14 associated, as compared to Cu, which was mainly associated with macromolecules.  
15  
16  
17  
18  
19  
20  
21  
22  
23  
24  
25  
26  
27  
28  
29

30 Worms et al. [18] applied AF4-ICP-MS to examine the association of metals  
31 to the colloidal organic matter from wastewater treatment plant. The colloidal organic  
32 matter was classified into low molecular mass and high molecular mass fractions.  
33 Most metals, including Ag, Cd, Cu, Cr, Mn and Zn, were found associated only with  
34 the low molecular mass fraction, suggesting that the low molar mass fraction of the  
35 colloidal pool played a key role in controlling the distribution of metals in the  
36 colloidal phase. The exceptions included Al, Fe and Pb, which were found to be also  
37 associated with the high molecular mass fraction.  
38  
39  
40  
41  
42  
43  
44  
45  
46  
47

48 Krachler et al. [19] applied the coupling of AF4 with ICP-MS to characterize  
49 colloidal iron carriers in peat-draining rivers in North Scotland. The size distribution  
50 of natural organic matter determined by FFF-UV ( $\lambda=220 \text{ nm}$ ) was merged with Fe  
51 distribution by AF4-ICP-MS. The distribution of Fe was bimodal. The smaller  
52 particle size indicated iron complexed by natural organic matter. The second peak  
53  
54  
55  
56  
57  
58  
59  
60

1  
2  
3 was higher representing the more abundance of Fe, which might be iron oxides.  
4  
5 However, for river with high sodium concentration, the signal of secondary Fe species  
6  
7 became lower, implying that these iron species were more vulnerable to increase in  
8  
9 salinity.  
10

11 Plathe et al. [20] coupled AF4 to high-resolution ICP-MS to study  
12 relationships between trace metals and nanoparticles in contaminated sediment. The  
13 signal of several elements including Al, Fe, Si, Mg, Ti, Zn, Cu, Mn, Ba, Pb, Sr, Cr, Ce,  
14 La, Co, Th, Bi, Pr, and In were monitored. Al and Si represented the peak maximum  
15 at particle size larger than 100 nm. Peak maximum of Fe was at the particle size  
16 smaller than 100 nm. The peak maximum of Ti was between that of Al and Fe. The  
17 fractograms of Zn, Cu, and Pb were similar to that of Fe and Ti, implying that these  
18 elements were held on or in nanoparticle minerals containing Fe and Ti as major  
19 elements. The Al-rich minerals were much more depleted in the nanometer size  
20 fraction and showed less important role in metal binding.  
21  
22  
23  
24  
25  
26  
27  
28  
29  
30  
31  
32  
33

34 Neubauer et al. [21] investigated the effects of ionic strength and sample  
35 loading on the retention and recovery for size characterization of natural nanoparticles  
36 by AF4 coupled with ICP-MS. Wide range of polystyrene sulfonate (PSS) molecular  
37 weight standards of 1100-145000 g mol<sup>-1</sup> were used to cover particle size range of  
38 natural organic matter and its aggregates. To obtain reliable results, higher ionic  
39 strength carrier solution with lower sample loading were recommended. Ammonium  
40 carbonate/ammonium carbamate solution was used as a carrier liquid due to its  
41 interference-free ICP-MS property. The Rh solution was added as an internal  
42 standard for ICP-MS detection. From the UV-vis fractogram, natural organic matter  
43 appeared only one peak, which could bind with about 50% of Fe. However, two  
44  
45  
46  
47  
48  
49  
50  
51  
52  
53  
54  
55  
56  
57  
58  
59  
60

1  
2  
3 peaks were observed in the Fe fractogram, by which the other peak of Fe was defined  
4  
5 as iron-rich nanophase.  
6

7  
8 Claveranne-Lamolère et al. [22] exploited AF4-ICP-MS together with CE-  
9  
10 ICP-MS coupling to characterize uranium–colloid interactions. With AF4-ICP-MS,  
11  
12 the colloidal population in soil leachates appeared to be polydisperse, which was  
13  
14 identified as aggregates probably constituted of inorganic colloidal Ti, Mg, Ca, Fe,  
15  
16 Al-rich and carbon-based particles as well as organic matter. Uranium was associated  
17  
18 with the whole colloidal population. Then, CE-ICP-MS was employed to examine  
19  
20 the effect of pH on the affinity between uranium and colloid surface sites.  
21  
22

23  
24 Brittain et al. [23] studied the chemical speciation of U and trace metals in  
25  
26 depleted uranium (DU) contaminated soils. Soil samples were extracted with sodium  
27  
28 pyrophosphate to remove the organic-bound fraction followed by a further  
29  
30 chemical extraction to separate humic and fulvic complexes. The majority of  
31  
32 elements (Mn, Fe, Cu, Zn) gave monomodal fractograms for the soils studied, with  
33  
34 the exception of Pb and U. Bimodal distribution was found for Pb in the sodium  
35  
36 pyrophosphate extract of the Kirkcudbright soil, but Pb exhibited monomodal  
37  
38 distribution in the fulvic and humic acid fractions. In the control soil, U was  
39  
40 primarily associated with the sodium pyrophosphate fraction with only a small  
41  
42 amount of U associated with the humic acid fraction, whereas negligible amount of U  
43  
44 was found in the fulvic acid fraction. In the Eskmeals soil, U displayed a monomodal  
45  
46 peak in the sodium pyrophosphate fraction, and in the isolated humic fraction,  
47  
48 whereas a bimodal peak was observed for the fulvic acid fraction.  
49  
50

51  
52 Henderson et al. [24] exploited FIFFF-ICP-MS to characterize nanoparticles  
53  
54 release during anoxia in grassland soils receiving biannual broiler litter amendments  
55  
56 in 12 of the last 15 years. Bimodal distribution was observed at a very small size  
57  
58  
59  
60

1  
2  
3 fraction and at approximately 400 nm particles or aggregates. High concentrations of  
4 Al and Si were found in these fractions with minor contributions from Fe and Ti. The  
5 peak of Fe corresponded well with peaks of Si and Al, whereas the peak of Ti was  
6 shifted toward later elution times. Nonetheless, P exhibited an elution peak slightly  
7 earlier than those of Si, Al, and Fe.  
8  
9

10  
11  
12  
13  
14 Saito et al. [25] employed FIFFF-ICP-MS to examine size distributions and  
15 elemental compositions of nano-colloids in the granitic groundwater. Owing to the  
16 relatively low concentration of colloids groundwater, three-step enrichment of  
17 colloids was carried out by ultrafiltration, the focusing technique with a large sample  
18 injection loop, and the slot flow technique. In most cases, the size distributions of Al,  
19 Mg, and Lu were corresponded well with that of organic colloids. Similarly, most of  
20 other lanthanide and actinide elements were also shown to be associated with organic  
21 colloids, but with smaller size fractions. Sr was found to be associated with Ca-  
22 dominant fraction, which might be forming solid solution in  $\text{CaCO}_3$ .  
23  
24  
25  
26  
27  
28  
29  
30  
31  
32  
33

34 The group of Stolpe reported various examples of FFF-ICP-MS to examine  
35 metal binding with environmental colloids [26-28]. They applied on-line coupling of  
36 FIFFF to detectors including UV-absorbance, fluorescence, and ICP-MS to examine  
37 Fe, P, Mn, Cu, Zn, Pb, and U distributions along with 'nanocolloidal size distributions'  
38 (0.5– 40 nm, hydrodynamic diameter) of chromophoric and fluorescent organic  
39 matter in the Mississippi river, Pearl river, and the northern Gulf of Mexico [26]. The  
40 distributions of Cu and U in all rivers were monomodal in the 0.5–4 nm size range,  
41 matching the UV254 size spectrum. In Pearl river, Zn also showed similar  
42 distribution with those of Cu and U, but with a broader peak extending into the size  
43 larger than 5 nm. For Mn and Pb, the distributions were similar to that of Fe which  
44 showed an additional peak in the 5–25 nm size range, in comparison with those of Cu  
45  
46  
47  
48  
49  
50  
51  
52  
53  
54  
55  
56  
57  
58  
59  
60

1  
2  
3 and U. The distribution of P resembled that of Fe in Pearl river, with P distributed in  
4 both the 0.5–4 nm and the 5–25 nm peak. In Mississippi river, on the other hand, it  
5 resembled those of Cu and U, by which only the 0.5–4 nm peak could be  
6 distinguished.  
7  
8  
9  
10

11 Further, the technique was also employed to examine Cr, Mn, Fe, Co, Ni, Cu,  
12 Zn, and Pb distributions along with ‘nanocolloidal size distributions’ (0.5– 40 nm,  
13 hydrodynamic diameter) of humic-type and chromophoric dissolved organic matter  
14 (CDOM) in Alaskan rivers [27]. Similar to UV254 absorbance, carbon, and Fe  
15 distributions, during the spring flood, Cr, Co, Cu, Ni, Mn, Zn, and Pb showed one  
16 single peak centered at 1.5 nm, and were largely found in the 0.5–4 nm size fraction.  
17 During the summer, Cr, Co, Cu, and Ni showed the sharp peak at 1.5 nm, but with a  
18 narrower 0.5–3 nm width than during spring flood. For the other elements, their  
19 signals were too low to be observed.  
20  
21  
22  
23  
24  
25  
26  
27  
28  
29  
30  
31

32 In another application, Stolpe et al. [28] used flow FFF-ICP-MS to  
33 characterize the binding between nanocolloids (0.5 – 40 nm) with Fe, La, Ce, Pr, Nd,  
34 Sm, Gd, Tb, Dy, Ho, Er, Tm, Yb and Lu in six Alaskan rivers in the Yukon River  
35 basin. Seasonal changes and rivers affected on REE-binding of the nanocolloids.  
36 Nanocolloids were classified as ‘fulvic-rich’, ‘organic/iron-rich’ and ‘iron-rich’  
37 fractions. During the spring flood, REEs were high in concentration and were largely  
38 associated with <8 nm organic/iron-rich nanocolloids. During summer base flow, the  
39 concentrations of REEs were low and REEs were mostly associated with small  
40 (<0.5 nm) organic and/or carbonate complexes, probably leached from deeper soil  
41 layers.  
42  
43  
44  
45  
46  
47  
48  
49  
50  
51  
52  
53  
54  
55

### 56 **Inorganic nanoparticles**

57  
58  
59  
60

1  
2  
3 With the emergence of nanotechnology, the use of nanoparticles has increased  
4 tremendously. Inorganic nanoparticles can be detected by FFF-ICP-MS. This review  
5 highlights some selected applications of FFF-ICP-MS to various types of inorganic  
6 nanoparticles, including silver (AgNPs), gold (AuNPs), titanium dioxide (TiO<sub>2</sub>), and  
7 other inorganic nanoparticles.  
8

9  
10  
11  
12  
13  
14 Bednar and coworkers [29] compared the sensitivity and selectivity obtained  
15 by various instruments (UV, DLS, ICP-MS, ICP-DRC-MS, and ICP-AES) as an on-  
16 line detection system for FFF. In their work, several types of inorganic nanoparticles  
17 were investigated, including AgNPs, AuNPs, and quantum dots. Among the detection  
18 techniques studied therein, ICP-MS and ICP-AES provided specific and simultaneous  
19 detection for AgNPs with detection limit of 10 µg L<sup>-1</sup> and 100 µg L<sup>-1</sup>, respectively.  
20 For UV detection, even the detection limit of 100 µg L<sup>-1</sup> was achieved, the technique  
21 was not specific and could not differentiate between nanoparticles from different  
22 elements. For the DLS technique, the detection limit was as high as 1500 µg L<sup>-1</sup>.  
23 Moreover, the impurities in the suspension or a few large particles skewed the DLS  
24 measurement to a larger size. Therefore, the advantages of ICP-MS and ICP-AES as  
25 an on-line detection system were emphasized and applied to detect multiple  
26 components of nanoparticle systems, including core– shell gold–silver nanoparticles,  
27 Cd–Se–Zn–S quantum dots, and silver nanoparticles after sulfidation.  
28  
29  
30  
31  
32  
33  
34  
35  
36  
37  
38  
39  
40  
41  
42  
43  
44

45  
46 The mixtures of 10, 30, and 60 nm AuNPs with 10, 30, and 60 nm AgNPs  
47 were separated by FFF with different detection techniques (UV, DLS, ICP-MS, and  
48 ICP-AES). ICP-MS provided the lowest detection limit at 10 µg L<sup>-1</sup> for both AuNPs  
49 and AgNPs compared with ICP-AES (200 µg L<sup>-1</sup> for AuNPs and 100 µg L<sup>-1</sup> for  
50 AgNPs), UV (400 µg L<sup>-1</sup> for AuNPs and 100 µg L<sup>-1</sup> for AgNPs), and DLS (4,000 µg  
51 L<sup>-1</sup> for AuNPs and 1,500 µg L<sup>-1</sup> for AgNPs).  
52  
53  
54  
55  
56  
57  
58  
59  
60

1  
2  
3 ICP-MS, ICP-DRC-MS, and ICP-AES were coupled with FFF for  
4 characterization of cadmium selenide-zinc sulfide core-shell quantum dots (CdSe-  
5 ZnS). For Cd and Zn, ICP-MS provided more detection capabilities over ICP-AES.  
6  
7  
8  
9  
10 However, sulfur could not be detected by standard mode ICP-MS (polyatomic  
11 interferences), whereas ICP-AES could measure sulfur. Moreover, DRC was used to  
12 overcome interferences for sulfur and selenium detection.  
13  
14  
15  
16  
17

### 18 *Silver nanoparticles*

19  
20  
21 Hoque et al. [30] reported the use of AF4 with on-line and off-line ICP-MS for  
22 size characterization and quantitative analysis of AgNPs in aqueous matrices. For  
23 online AF4-ICP-MS, indium was selected as an internal standard to correct for signal  
24 drift during separation and analysis. External calibration was carried out by injecting  
25 a series of AgNPs standard into AF4 system with ICP-MS detection. With this online  
26 detection procedure, LOQ of  $1.4 \text{ ng mL}^{-1}$  (0.1 mL injection volume), LOD of  $0.8 \text{ ng}$   
27  $\text{mL}^{-1}$  were obtained. Three calibration approaches for quantification of AgNPs in  
28 water samples were evaluated. These include the external calibration with AgNPs  
29 standards, standard addition of AgNPs in the samples injected into the AF4 channel,  
30 and flow injection approach using dissolved  $\text{Ag}^+$  standard introduced into the eluent  
31 flow after the AF4 system via an on-line injector. The first two approaches provided  
32 information on both particle size and concentration, whereas only the information on  
33 concentration was obtained from the last approach. Application of the three  
34 calibration approaches to a wastewater sample displayed good agreement between  
35 the external and standard addition calibration approaches. However, the flow  
36 injection approach gave different values, which might be due to the presence of  
37 various other insoluble forms of silver (e.g.,  $\text{Ag}_2\text{S}$  and  $\text{AgCl}$ ) rather than AgNPs.  
38  
39  
40  
41  
42  
43  
44  
45  
46  
47  
48  
49  
50  
51  
52  
53  
54  
55  
56  
57  
58  
59  
60

1  
2  
3 Ulrich and coworkers [31] stated the importance of sample handling and  
4 preparation on nanoparticle analysis. They studied the effect of dilution, pH, ionic  
5 strength on nanoparticle analysis. Two types of nanosilvers were used in this study;  
6 AgNPs with citrate stabilized (Ag@citrate, electrostatic stabilization) and AgNPs  
7 with PVA stabilized (Ag@PVA, steric stabilization). With sample dilution,  
8 increasing of particle size was observed for both types of AgNPs, which might be due  
9 to an alteration of the ratio between nanoparticle and coating or functionalization  
10 agent bound to its surface. The effect of ionic surfactant or electrolyte addition into  
11 the carrier liquid was also investigated. Adding sodium nitrate into the carrier liquid  
12 resulted in increasing in size of both types of silver nanoparticles. The authors  
13 suggested that addition of ions might change the electrostatic force between coating  
14 or functionalization agent and nanoparticle core, which in general the sterically  
15 stabilized nanoparticles should be less sensitive to ionic strength changes than the  
16 electrostatically stabilized ones. Similarly, the effect of pH changes was more impact  
17 on the electrostatically stabilized than the sterically stabilized nanoparticles. The time  
18 dependent curves showing the change in particle size upon pH change implied the  
19 kinetics of the agglomeration behavior. For Ag@PVA a relatively steep increase was  
20 observed after 120 minutes, whereas it took only after 60 minutes for Ag@citrate.  
21 Moreover, the charge of nanoparticles also affected on separation efficiency and  
22 recovery rate in FFF-ICP-MS analysis. Shift in the retention time might be expected  
23 with different particle-membrane interaction.  
24  
25  
26  
27  
28  
29  
30  
31  
32  
33  
34  
35  
36  
37  
38  
39  
40  
41  
42  
43  
44  
45  
46  
47  
48

49 Bolea et al. [32] reported the hyphenated techniques of AF4 and ICP-MS for  
50 the characterization and quantification of AgNPs standards and AgNPs in consumer  
51 products. Various parameters including the mobile phase composition (pH, ionic  
52 strength, and the presence of surfactants), the injection/focusing time, and the  
53  
54  
55  
56  
57  
58  
59  
60

1  
2  
3 crossflow were optimized. Different compositions of nonionic (Tween 20) and ionic  
4 surfactants (SDS) were compared in term of the colloid stabilization based on the  
5 steric and electrostatic repulsion. Nonionic surfactant offered the shorter time elution  
6 peak with narrower profile, which might be due to weaker repulsion forces among  
7 AgNPs, and thereby the particles were focused into a narrow area. Nonetheless, with  
8 nonionic surfactant, three different AgNPs standards (10, 20, and 80 nm) eluted at the  
9 same retention times, suggesting that nonionic surfactant was not an appropriate  
10 carrier liquid under this condition. In contrast, ionic surfactant promoted electrostatic  
11 repulsion forces, leading to longer retention times of the AgNPs. The best sample  
12 recovery for all AgNPs standards was observed when 0.01% SDS at pH 8 was used as  
13 a carrier liquid. Increasing ionic strength of the carrier liquid led to the reduction in  
14 sample recovery, as the repulsion between AgNPs and the membrane surface was  
15 shielded, leading to nanoparticle adsorption on the membrane surface. With ultrapure  
16 water as a carrier liquid, conditioning of the membrane surface was necessary by  
17 repeated injections of concentrated AgNPs to reduce adsorption, by which recoveries  
18 of  $98\pm 5\%$  were obtained when four injections of AgNPs were applied to condition the  
19 membrane. Between the two commonly used membranes, poly(ethersulfone) or PES  
20 membrane provided higher recovery for AgNPs, as opposed to regenerated cellulose  
21 membrane. With optimum condition, FFF channel calibration was performed by  
22 using various AgNPs standards with the particle size between 10 to 80 nm, and  
23 consequently the method was applied to characterize particle size of AgNPs in  
24 antiseptic and dietary supplement. For element detection and quantitation purpose,  
25 ICP-MS was used. The results obtained from direct nebulization were agreeable with  
26 those from the digested sample analysis.  
27  
28  
29  
30  
31  
32  
33  
34  
35  
36  
37  
38  
39  
40  
41  
42  
43  
44  
45  
46  
47  
48  
49  
50  
51  
52  
53  
54  
55  
56  
57  
58  
59  
60

1  
2  
3 Poda et al. [33] reported the use of FFF-ICP-MS for characterization of  
4 AgNPs mixture and applied to biological media samples. In their work, a  
5 symmetrical FIFFF equipped with 10 kDa regenerated cellulose membrane was used  
6 with 0.025% FL-70 in the presence of 0.025% sodium azide as carrier liquid. NIST-  
7 traceable polystyrene bead size standards (20, 50, and 100 nm) were used for FIFFF  
8 channel calibration. The recoveries of 88-89% were obtained for the three sizes of  
9 AgNPs at 10, 40 and 70 nm. The recovery of less than 100% might be due to the  
10 interaction of particles with FFF membrane and particle loss during ICP-MS sample  
11 introduction. The sizes of AgNPs obtained from FFF analysis agreed well with the  
12 results from DLS, but larger than the TEM sizes, reflecting that the FFF and DLS  
13 techniques measure the hydrodynamic particle rather than the primary particle size.  
14 Injection of a mixture containing 10, 40, and 70 nm AgNPs at concentrations of  
15  $67 \mu\text{g L}^{-1}$  showed clearly defined peaks, although baseline resolution was not  
16 achieved. With increase in particle size, the noise signals were significantly increased.  
17 The authors hypothesized that this might be due to the delivery of larger amounts of  
18 Ag per particle unit into the plasma/detector system. At the concentration down to  
19  $6.7 \mu\text{g L}^{-1}$  of mixed AgNPs, three peaks were quite noisy, but still sufficiently defined.  
20 However, increasing the cross flow from 1 to  $1.1 \text{ mL min}^{-1}$  improved the peak  
21 separation with minimal reducing sensitivity and minor peak broadening. In addition,  
22 the study of biota exposure to AgNPs was carried out. The freshwater oligochaete,  
23 *Lumbriculus variegates*, was exposed to PVP-coated AgNPs spiked sediment. The  
24 tissues were extracted after 28 days exposure by deionized water using sonication.  
25 The authors found that AgNPs became bigger at 46 nm after biological exposure  
26 compared to the original size of 31 nm, which might be resulted from coating of the  
27 particles with proteins or other biological molecules. Alternatively, the PVP coating  
28  
29  
30  
31  
32  
33  
34  
35  
36  
37  
38  
39  
40  
41  
42  
43  
44  
45  
46  
47  
48  
49  
50  
51  
52  
53  
54  
55  
56  
57  
58  
59  
60

1  
2  
3 might be removed as a result of biological mechanisms or abiotic reactions in the soil  
4 exposure medium, resulting in aggregation of the destabilized silver particles.  
5  
6

7  
8 Coleman and coworkers [34] used FFF-ICP-MS to examine the effects of  
9 particle size and the coating on the bioaccumulation and depuration of AgNPs within  
10 the gut cavities of aquatic invertebrates (*L. variegates*). Prior analysis, the *L.*  
11 *variegatus* was homogenated and sonicated for 1 h in deionized water. After 48 h of  
12 depuration, FFF-ICP-MS fractograms showed a fraction of AgNPs which were  
13 smaller in size than the original particle sizes. This result was agreeable with the data  
14 from single particle (SP)-ICP-MS analysis performed for the collected fractions from  
15 FFF. The analysis of the collected fractions at the shouldered void peaks from FFF  
16 with the SP-ICP-MS revealed that this fraction could be either dissolved Ag, small  
17 particles, or Ag associated with organic moieties, such as proteins recovered from the  
18 tissue with water sonication extraction. However, all dissolved Ag should be  
19 removed by cross flow and filtered off through the membrane before reaching the  
20 detector. This study illustrated that with FFF-ICP-MS and SP-ICP-MS, AgNPs could  
21 be retained in the *L. variegatus* for longer than the standard 6 h depuration period, as  
22 indicated in the recommended procedure by USEPA for bioaccumulation testing.  
23  
24  
25  
26  
27  
28  
29  
30  
31  
32  
33  
34  
35  
36  
37  
38  
39

40  
41 Another work by Poda et al. [35] was to examine the effect of UV irradiation  
42 on the stability of AgNPs using FFF-ICP-MS. The 50 nm polyvinylpyrrolidone-  
43 capped AgNPs in the presence and absence of dissolved organic carbon (DOC) were  
44 examined. AgNPs were prepared in three different media, including deionized (DI)  
45 water, moderately hard reconstituted water (MHW), and MHW with DOC. The ICP-  
46 MS response of AgNPs in MHW was decreased when compared with AgNPs in DI  
47 water, as MHW triggered particle aggregation by charge neutralization. However,  
48 adding 4 mg L<sup>-1</sup> DOC solution in the MHW caused the increase in the ICP-MS signal,  
49  
50  
51  
52  
53  
54  
55  
56  
57  
58  
59  
60

1  
2  
3 as the DOC solution consisted of negatively charged carboxylates that increased  
4 nanoparticle dissolution by scavenging and complexing  $\text{Ag}^+$  and possibly reducing  
5  $\text{Ag}^+$  to  $\text{Ag}^0$ . To mimic 24 h exposure of AgNPs to sunlight, photolysis with sixteen  
6  
7  
8  
9  
10 14 W black lamps was set up for approximately 1 h. The photolysis resulted in a  
11 decrease in average particle size of AgNPs, which might be due to the photo-induced  
12 oxidation of the PVP and dissolution of metallic silver. Moreover, it was observed  
13 that particle size of AgNPs in MHW and DOC/MHW were also decreased after  
14 photolysis reaction. Not only particle size was decreased after adding DOC  
15 component in AgNPs solution, the overall particle concentration was also decreased,  
16 which might be caused by the oxidation of silver to  $\text{Ag}_2\text{O}$  followed by dissolution. In  
17 addition, the toxicity of AgNPs under light exposure was investigated using the  
18 standard zooplankton model.  
19  
20  
21  
22  
23  
24  
25  
26  
27  
28

29  
30 Loeschner et al. [36] developed a method based on the use of AF4-ICP-MS  
31 for the analysis of AgNPs in chicken meat. To mimic a possible scenario where  
32 AgNPs may migrate from an antibacterial food packaging material into meat, AgNPs  
33 stabilized with polyvinylpyrrolidone (PVP) were spiked into chicken meat. Then,  
34 enzymolysis by Proteinase K for 40 min at 37 C of the homogenized AgNPs spiked  
35 chicken meat sample was performed to degrade protein to peptides and amino acids.  
36 The fractogram of the enzymatically digested meat sample containing AgNPs  
37 displayed one large peak with two smaller peaks eluting close to the void volume.  
38 The large peak was assigned to AgNPs which eluted earlier than the pristine AgNPs  
39 without meat. This earlier elution hampered the accurate determination of the particle  
40 size distribution based on retention times.  
41  
42  
43  
44  
45  
46  
47  
48  
49  
50  
51  
52

53  
54 Bolea et al. [37] applied AF4-ICP-MS for investigation of changes in AgNPs  
55 particle size incubated in culture medium and cells to gain an insight into nanotoxicity.  
56  
57  
58  
59  
60

1  
2  
3 Particle size of AgNPs was bigger than the original size upon incubation in the culture  
4 medium, suggesting the occurrence of protein corona formation around the AgNPs.  
5  
6  
7 Using the operating condition to accommodate protein fractionation (19, 53, 113 kDa),  
8  
9  
10 Ag signals appeared at the same retention time as the proteins suggesting that AgNPs  
11  
12 were partially oxidized to  $\text{Ag}^+$  which could associate with proteins present in the  
13  
14 culture medium. The association of AgNPs with HepG2 cells was examined by using  
15  
16 AF4-ICP-MS after alkaline solubilization. The fractograms revealed the presence of  
17  
18 AgNPs, but with a smaller size than the original size, implying that a dissolution  
19  
20 process might occur. However, the presence of AgNPs peak provided the evidence of  
21  
22 AgNPs association with the cells.  
23  
24  
25  
26

### 27 ***Gold nanoparticles***

28  
29 Schmidt et al. [38] reported the use of FFF coupled with ICP-MS for  
30  
31 separation and quantification of 10, 20, and 60 nm AuNPs mixtures. The mean  
32  
33 recoveries of 50%, 95%, and 67% were observed for 10, 20, and 60 nm AuNPs,  
34  
35 respectively. The incomplete recoveries were due to possible adhesion of AuNPs on  
36  
37 the membrane surface during separation process. The limits of detection were varied  
38  
39 between 0.02 ng Au to 0.4 ng Au depending on nanoparticle diameter. The LODs  
40  
41 were increased with increasing particle size. AuNPs of 10 nm and/or 60 nm were  
42  
43 injected to sixteen female Wistar rats. After 24 h, the livers were taken out and  
44  
45 solubilized in tetramethylammonium hydroxide. With ICP-MS detection using Rh as  
46  
47 an internal standard after microwave assisted wet ashing, the recoveries of AuNPs  
48  
49 from rat livers were ranging from 86% to 123% of their total Au content. However,  
50  
51 the 10 nm or 60 nm AuNPs could not be observed by FFF owing to the association of  
52  
53 AuNPs with remains of liver tissue.  
54  
55  
56  
57  
58  
59  
60

1  
2  
3 Gray et al. [39] compared the performances of hydrodynamic chromatography  
4 (HDC) and AF4 coupled with ICP-MS for the analysis of AuNPs. The resolution,  
5 recovery, and detection limit obtained by the two techniques were evaluated. Two  
6 types of AuNPs, which were tannic stabilized- and citrate stabilized-AuNPs of 5, 20,  
7 50, and 100 nm, were examined. The resolution obtained from HDC was poorer than  
8 that from AF4, despite the fact that better resolution of AF4 over HDC came with the  
9 drawbacks of longer run time. With both techniques, different surface coating on the  
10 AuNPs showed variability in the relationship between time and diameter under  
11 identical operating conditions, implying that size calibration should be performed by  
12 using the particles with coatings that caused a similar retention behavior to that of the  
13 unknown sample. This problem should be paid great attention as in the  
14 environmental or biological systems, NPs were likely to accumulate coatings on their  
15 surface. Considering the sample recovery during separation process, HDC provided  
16 higher recovery than AF4 as particle sorption on the separation membrane was the  
17 main cause of sample loss. The limits of detection for both techniques were  
18 approximately  $5 \mu\text{g L}^{-1}$ .  
19  
20  
21  
22  
23  
24  
25  
26  
27  
28  
29  
30  
31  
32  
33  
34  
35  
36  
37  
38  
39  
40

#### 41 *Titanium dioxide nanoparticles*

42  
43 Owing to its several interesting properties, i.e., insoluble; high stable;  
44 nonreactive; thermally stable; nonflammable; low cost; and environmental friendly,  
45  $\text{TiO}_2$  nanoparticles are used in many applications. Various research groups reported  
46 the use of FFF with element specific detectors for size characterization of  $\text{TiO}_2$   
47 nanoparticles, particularly in cosmetic products.  
48  
49  
50  
51  
52  
53

54 In 2008, Contado and Pagnoni applied FFF with off-line ICP-AES detection  
55 for size characterization of  $\text{TiO}_2$  in commercial sunscreen lotion [40].  $\text{TiO}_2$  particles  
56  
57  
58  
59  
60

1  
2  
3 showed a strong affinity for each other and, in some cases, even for the accumulation  
4 wall of the FIFFF channel (membrane). In the case of commercial sample, Ti  
5 concentration profiles obtained by ICP-AES were agreeable with those from the UV  
6 detector. The authors mentioned that different sunscreen formulations required  
7 different sample preparation methods. In 2010, the same researchers proposed the use  
8 of square wave voltammetry as a lower cost technique to quantify the Ti  
9 concentration in commercial foundation creams [41]. In their study, the results  
10 obtained from the square wave voltammetry were compared with ICP-AES. With  
11 square wave voltammetry, the presence of interfering elements, such as  $\text{Pb}^{2+}$  and  $\text{Cu}^{2+}$   
12 resulted in the unexpectedly lower values of Ti concentration as compared to the  
13 values obtained by ICP-AES. Therefore, ICP-AES was used as an off-line detector  
14 for the fractions collected from FFF. Furthermore, SdFFF and FIFFF were used to  
15 investigate the size of  $\text{TiO}_2$  nanoparticles in the commercial foundation creams after  
16 solvent extraction. The mixture of water : methanol : hexane as a ratio of 1 : 4 : 1 was  
17 an optimum extractant because the higher amount of methanol better dispersed the  
18 foundation, and was evaporated more rapidly than water. With SdFFF analysis, the  
19 void peaks for all six concentrated suspension samples were significantly high, which  
20 might be contributed from some particles with size smaller than 100 nm or bigger size  
21 with density lower than  $4 \text{ g mL}^{-1}$ . To analyze the smaller particle size fraction, FIFFF  
22 was employed and this sub-technique was density independent. With FIFFF, particles  
23 of about 2-3 nm and about 15 nm were detected in the samples.  
24  
25  
26  
27  
28  
29  
30  
31  
32  
33  
34  
35  
36  
37  
38  
39  
40  
41  
42  
43  
44  
45  
46  
47  
48

49  
50 Samontha et al. [42] reported the coupling between SdFFF and ICP-MS for  
51 size characterization of  $\text{TiO}_2$  nanoparticles in sunscreen samples after hexane  
52 extraction to remove organic components from the samples. Sunscreen products of  
53 various sun protection factor (SPF) values were used as samples. The particle size  
54  
55  
56  
57  
58  
59  
60

1  
2  
3 distributions of titanium dioxide in most sunscreen samples investigated in this work  
4  
5 were larger than 100 nm, which might be attributed to the secondary particles. The  
6  
7 authors also carried out quantitative analysis of titanium in the samples by comparing  
8  
9 the results obtained from the on-line SdFFF-ICP-MS and those from the off-line ICP-  
10  
11 MS determination of titanium after acid digestion. The concentrations of titanium  
12  
13 found from both methods were in good agreement.  
14  
15

16 Nischwitz and Goenaga-Infante [43] described the first systematic comparison  
17  
18 and optimization of extraction methods for titanium dioxide nanoparticles in  
19  
20 sunscreen samples. They used FIFFF with on-line ICP-MS for size characterization  
21  
22 of titanium dioxide nanoparticles in sunscreens after defatting of the sample with  
23  
24 hexane followed by bath sonication with an aqueous extractant. With this extraction  
25  
26 procedure, stable suspensions of secondary titanium dioxide particles were obtained.  
27  
28 To obtain the primary particle size, further addition of a small amount of hexane to  
29  
30 the aqueous extractant was recommended to disaggregate the particles. The  
31  
32 developed sample preparation procedure prior to FFF-ICP-MS was applied to analysis  
33  
34 of commercial sunscreens with various sun protection factors.  
35  
36  
37

38 Another recent published work on the use of AF4-ICP-MS for TiO<sub>2</sub>  
39  
40 nanoparticles analysis in cosmetic and food products is given by López-Heras et al.  
41  
42 [44]. In their work, the experimental parameters affecting NPs separation and  
43  
44 elemental quantification by AF4-UV/ICP-MS were optimized and discussed.  
45  
46 Polystyrene latex standards of three known sizes (22, 54, and 100 nm) were used as  
47  
48 calibrants. However, by collecting the fractions analyzed by AF4 to further  
49  
50 characterize by TEM, it was found that erroneous results might be obtained when  
51  
52 using the latex standards for calibrating rutile TiO<sub>2</sub> NPs size, due to the high  
53  
54 aggregation state of TiO<sub>2</sub>. To reduce agglomeration, the use of ultrasound energy was  
55  
56  
57  
58  
59  
60

1  
2  
3 explored. Then, AF4-ICP-MS was applied to detect TiO<sub>2</sub> NPs in moisturizing cream,  
4  
5 sugar glass, and coffee cream. However, Ti signal was negligible in food extracts,  
6  
7 suggesting that although TiO<sub>2</sub> was commonly used as anti-caking agent and food  
8  
9 additive, the compound might not be present as NPs.  
10

11  
12 Ulrich and coworkers [31] examined the effects of pH, ionic strength, and  
13  
14 dilution on the analysis of polyacrylate functionalized TiO<sub>2</sub> nanoparticles. The size of  
15  
16 TiO<sub>2</sub> nanoparticles was not significantly changed after 1:50, 1:100, 1:500, 1:1000, and  
17  
18 1:5000 dilution. The change of TiO<sub>2</sub> particle size was also insignificant by changing  
19  
20 ionic strength with sodium nitrate addition. Nonetheless, pH change affected on the  
21  
22 particle size of TiO<sub>2</sub> nanoparticles. In this case, hydrolysis or the other chemical  
23  
24 interactions could influence on crosslinking or binding between polymer coating  
25  
26 component of TiO<sub>2</sub> nanoparticles stabilized by polyacrylate.  
27  
28  
29  
30  
31  
32

### 33 ***Other inorganic nanoparticles***

34  
35 Pace et al. [45] applied FIFFF-ICP-MS for characterization of four CdSe/ZnS  
36  
37 quantum dots including 2 nm QDs (green-emitting) and 5 nm QDs (red-emitting) with  
38  
39 two different surface coatings, i.e., polyethylene oxide (PEO); and 11-  
40  
41 mercaptoundecanoic acid (MUA). The isotopes monitored included <sup>64</sup>Zn, <sup>82</sup>Se, and  
42  
43 <sup>114</sup>Cd using <sup>45</sup>Sc and <sup>209</sup>Bi as internal standards for all the samples. However,  
44  
45 instrument drift during FIFFF-ICP-MS analysis was not observed. Therefore, all  
46  
47 elemental concentrations were not normalized by internal standard intensities. The  
48  
49 signals from <sup>64</sup>Zn, <sup>82</sup>Se, and <sup>114</sup>Cd exhibited similar hydrodynamic diameters with the  
50  
51 size of 23, 24, 24, and 29 nm for red MUA, green MUA, red PEO, and green PEO  
52  
53 QDs, respectively. However, their elemental compositions were significantly  
54  
55 different. The MUA-coated QDs provided a very huge Cd signal compared to Se  
56  
57  
58  
59  
60

1  
2  
3 signal. The ratios of Cd/Se were 2.1, 23, 1.3, and 11 for red PEO, red MUA, green  
4 PEO, and green MUA QDs, respectively. These QDs were subjected to acute toxicity  
5 test by exposing to *Daphnia magna* for 48 h.  
6  
7  
8

9  
10 Huang et al. [46] incubated Be-associated materials in synthetic lung fluid  
11 (SLF) to study their dissolution and nanoparticle generation behaviors. To mimic  
12 inter- and intra- cellular environment in lung tissue, pH of SLF was adjusted to 4.5  
13 and 7.2, respectively. AF4-ICP-MS was utilized for size characterization of the  
14 particles in incubated samples from days 0, 4, 8, 32, 49, and 149. Cs was selected as  
15 internal standard for ICP-MS elemental quantification. The time-dependent  
16 dissolution and particle generation were investigated for Be(OH)<sub>2</sub> suspension (pH =  
17 4.5). No signals of Be, Al, and Si were detected in the size less than 450 nm for  
18 Be(OH)<sub>2</sub> suspensions on day 4 whereas they were found at 10-60 nm by day 32.  
19 However, the signal intensities of 10-60 nm particles were decreased whereas the  
20 larger particles were formed suggesting the presence of particle aggregation in SLF.  
21 Similar trend was observed at day 149. For all Be-associated materials (bertrandite-  
22 containing ore, beryl-containing ore, frit, Be(OH)<sub>2</sub>), they could significantly produce  
23 nanoparticles with the size distribution of 10-100 nm. However, less nanoparticles  
24 were observed for BeO, for which ionic Be were significantly produced after SLF  
25 incubation.  
26  
27  
28  
29  
30  
31  
32  
33  
34  
35  
36  
37  
38  
39  
40  
41  
42  
43  
44

45 M-M et al. [47] exploited FIFFF-ICP-MS to study particle size  
46 characterization of selenium nanoparticles stabilized by pectin, mixed alginate/pectin,  
47 ovalbumin, and β-lactoglobulin. Quantification of selenium was performed and  
48 indicated that a total of approximately 88–103% of the original selenium  
49 nanoparticles was detected during fractionation. These nanoparticles were subjected  
50 to incubation in gastrointestinal conditions, both in enzymatic and non-enzymatic  
51  
52  
53  
54  
55  
56  
57  
58  
59  
60

1  
2  
3 media. Particle size distributions shifted differently depending on the type of the  
4 stabilizing agent used in the preparation of selenium nanoparticles. Despite the shift  
5 in particle size distribution, more than 90% of selenium was still present in nanometer  
6 range after gastrointestinal digestion.  
7  
8  
9  
10

11 Heroult et al. [48] reported the use of AF4-ICP-MS together with multi-angle  
12 light scattering (MALS) and offline with transmission electron microscopy (TEM)  
13 with energy-dispersive X-ray analysis (EDAX) to perform size-based elemental  
14 quantification and size estimation of silica (SiO<sub>2</sub>) nanoparticles in coffee creamer.  
15 For optimization, SiO<sub>2</sub> of 12 nm was used and baseline separation was achieved with  
16 the cross flow rate of 2 mL min<sup>-1</sup>. Increasing the cross flow rate higher than  
17 2 mL min<sup>-1</sup> resulted in better separation with the expense of poorer recovery.  
18 Interestingly, the elution time of 12-nm SiO<sub>2</sub> was shorter than that of the 10-nm  
19 AuNPs calibrant. The authors hypothesized that the different elution behaviors  
20 between the two particles might be caused by differences in particle–membrane  
21 interactions between these particles. For the analysis of SiO<sub>2</sub> in coffee creamer,  
22 sample preparation was carried out by mixing the coffee creamer with water at  
23 different temperatures (40 °C and 60 °C) to mimic how the coffee was prepared in  
24 real life. Silicon fractograms obtained by FFF-ICP-MS for coffee creamer  
25 suspensions showed no significant effect of the water temperature on the particle size  
26 distribution of silica nanoparticles in coffee creamer extracts.  
27  
28  
29  
30  
31  
32  
33  
34  
35  
36  
37  
38  
39  
40  
41  
42  
43  
44  
45  
46  
47  
48  
49  
50  
51

### 52 **FFF-ICP-MS: concluding remarks and future challenge**

53

54 Field-flow fractionation-ICP-MS is regarded as a size-based elemental  
55 speciation tool, since it produces information on chemical composition across the size  
56  
57  
58  
59  
60

1  
2  
3 distribution of particulate and macromolecular samples. Various important  
4 applications of FFF-ICP-MS on size characterization of environmental colloids and  
5 nanoparticles were reviewed showing that the technique provides unique and new  
6 information, which cannot be gained otherwise. The technique shows great potential  
7 to revolutionize our understanding of trace metal-colloid interactions in  
8 environmental studies. The chemical composition as a function of particle size can be  
9 determined and adsorption characteristics can be investigated. Also, it provides  
10 information about bio-inorganic metal binding with macromolecules. The FFF-ICP-  
11 MS can be used to study the competitive binding of several metal ions to particular  
12 macromolecules. Regarding the engineered nanoparticles, applications of FFF-ICP-  
13 MS for the detection of inorganic nanoparticles in complex matrices, such as food or  
14 environmental samples, are useful. Further, FFF-ICP-MS can be used to gain more  
15 understanding of how nanoparticles interact with biological system, to provide the  
16 evidence of bioavailability and toxicity of nanoparticles.  
17  
18  
19  
20  
21  
22  
23  
24  
25  
26  
27  
28  
29  
30  
31  
32  
33

34 Considering the applications of FFF to nanoparticles, the difficulty is arisen  
35 from the variability in the retention behaviors of the same nanoparticle core with  
36 different coatings. Different particle/membrane interactions can cause shift in elution  
37 time of the same size particles, and also variation in sample recovery during  
38 separation process. The former leads to incorrect interpretation of particle size  
39 information, whereas the latter hinders the quantitative analysis of the nanoparticles.  
40 Solving these problems can be a challenge. To enable accurate interpretation of  
41 particle size, the use of single particle (SP)-ICP-MS in combination with FFF-ICP-  
42 MS is helpful. The works on FFF-ICP-MS with SP-ICP-MS can be found in several  
43 publications [34, 46, 49, 50], and many more publications on these techniques are  
44 expected. The use of matrix matched standard or the standard particles of the same  
45  
46  
47  
48  
49  
50  
51  
52  
53  
54  
55  
56  
57  
58  
59  
60

1  
2  
3 coating is suggested. Nonetheless, it is difficult to match the type of particle coating  
4  
5 between the standard and the unknown sample in practice. To overcome this problem,  
6  
7 we therefore propose the concept of matrix modification by addition of appropriate  
8  
9 amount of coating or stabilizing agent in the carrier liquid. The experiments to prove  
10  
11 this concept are now being conducted in our laboratory.  
12  
13

14 The main goals of analytical chemistry are identification and quantification.  
15  
16 Most FFF-ICP-MS works have reported only species identification. Although the  
17  
18 report on the quantitation by FFF-ICP-MS has been found, the quantitative  
19  
20 information has not been emphasized in most of the published articles. Elemental  
21  
22 speciation of macromolecular compounds is often involved with large carbon-rich  
23  
24 molecules [51, 52]. The presence of high carbon contents can hinder the accuracy of  
25  
26 trace element determination by ICP-MS. As previously reported, carbon  
27  
28 concentration of higher than 1,500 mg L<sup>-1</sup> could cause serious non-spectroscopic  
29  
30 interferences [53]. Although no clear evidence exists, varying compositions in  
31  
32 fractionated peaks influence the ionization efficiency in the plasma and therefore can  
33  
34 hinder exact external calibration of fractograms. The prohibitive factor to obtain  
35  
36 accurate quantification of elements in colloids or macromolecules is a lack of  
37  
38 standards. To obtain accurate quantitative information of trace elements bound to  
39  
40 macromolecules or particles, standards or standard reference materials must be  
41  
42 produced for a particular sample type. Alternatively a method, which can overcome  
43  
44 the matrix effects, must be used. Another clever way to achieve high accuracy is to  
45  
46 use ICP-isotope dilution MS (ICP-IDMS), where sources of systematic error are well  
47  
48 understood and can be controlled. Quantification by the isotope dilution analysis is  
49  
50 based on the measurement of an isotope ratio and not on the absolute ion intensity.  
51  
52 Application of an on-line FFF-ICP-IDMS should be considered by adopting the  
53  
54  
55  
56  
57  
58  
59  
60

1  
2  
3 concept of an on-line HPLC-ICP-IDMS suggested by Heumann et al. [54-59]. Two  
4 different spiking modes are possible, one using species-specific and another using  
5 species-unspecific spike solutions of isotope-enriched labeled compounds. The  
6 species-specific mode is only possible for element species well-defined in their  
7 structure and composition, whereas the species-unspecific mode could be applied in  
8 all cases where the structure and composition of the species are unknown. In the case  
9 of FFF-ICP-MS work, the latter approach, species-unspecific mode, is suggested.  
10 With the latter approach, equilibration of isotopes on line is not necessary. Instead of  
11 the HPLC column, the FFF channel can be used. This concept has been successfully  
12 demonstrated recently by Meermann et al.[60] for quantification of AgNPs. The on-  
13 line isotope dilution appears to be an ideal approach for accurate quantification of  
14 speciated elements. Nevertheless, the method is limited to only analyte elements with  
15 various sufficient isotopes. Monoisotopic elements (e.g., Al, As, Au, and Mn) cannot  
16 be quantified by this approach.  
17  
18  
19  
20  
21  
22  
23  
24  
25  
26  
27  
28  
29  
30  
31  
32  
33

34 Since the FFF-ICP-MS provides great merits and capabilities to solve  
35 important but unusual problems, analysts can expect to see more and more research  
36 works on this hyphenated technique. Collaborative work between analytical chemists  
37 and biochemists, biologists, botanists, and nutritionists is suggested. With the  
38 developed FFF-ICP-MS technique, the role of trace metals and their isotopes in  
39 nutrition, health and disease can be studied. With the use of enriched stable isotopes,  
40 differentiation between externally spiked elements and endogenous pools makes the  
41 investigation of the exchange between endogenous and exogenous elements of metal-  
42 containing macromolecules possible.  
43  
44  
45  
46  
47  
48  
49  
50  
51  
52  
53

54 In most of the FFF-ICP-MS publications, only SdFFF and FIFFF sub-  
55 techniques have been used. Coupling between EIFFF and ICP-MS may be seen in the  
56  
57  
58  
59  
60

1  
2  
3 future, as EIFFF has been shown able to separate nanoparticles [61, 62]. Since the  
4 separation in FFF is driven by physical force, less chemistry is involved in FFF  
5 compared to SEC or other chromatographic separations. To obtain elemental size  
6 separation without destroying the structure integrity of macromolecules or colloids,  
7 FFF-ICP-MS holds the best promise. Despite other advantages, FFF also suffers from  
8 limited separation resolution. Depending upon each FFF subtechnique, resolution  
9 might be improved by optimizing parameters governing fractionation power.  
10 Analytical chemists can expect to see multidimensional FFF, especially FFF-CE, add  
11 to the specificity of their elemental analyses. Multidimensional, hyphenated systems  
12 like FFF-CE-ICP-MS or FFF-HPLC-ICP-MS might be necessary to gain detailed  
13 information on clinical and environmental studies, where elemental size distribution  
14 and its functionality information are sought. This idea was demonstrated by  
15 Dubascoux et al. [63] to analyze the fractions collected from AF4 for further  
16 speciation analysis of organotin in environmental colloid by using off-line head-space  
17 solid-phase microextraction-gas chromatography with pulsed-flame photometric  
18 detection. The work on combination of FFF with other speciation techniques to  
19 provide more insightful information on elemental speciation should gain more interest.  
20 Looking to the future, FFF-ICP-MS can indeed offer a lot more as one might imagine.  
21 With our entrance into the “proteomics era”, it is essential to develop ideal assay for  
22 detection and quantification of proteins [64, 65]. The use of FFF-ICP-MS in  
23 combination with FFF and electrospray ionization mass spectrometry may be an  
24 additional approach for metalloproteomics.  
25  
26  
27  
28  
29  
30  
31  
32  
33  
34  
35  
36  
37  
38  
39  
40  
41  
42  
43  
44  
45  
46  
47  
48  
49  
50  
51  
52  
53  
54  
55

## 56 Acknowledgements

57  
58  
59  
60

1  
2  
3 The authors would like to acknowledge the Thailand Research Fund (TRF) for  
4 the research grants given to A. Siripinyanond and the scholarship given to P. M-M  
5 through the Royal Golden Jubilee Ph.D. Program (Grant No. PHD/0095/2553). We  
6 are also grateful for the financial support from the Office of the Higher Education  
7 Commission, Ministry of Education, Thailand through the Center for Innovation in  
8 Chemistry: Postgraduate Education and Research Program in Chemistry (PERCH-  
9 CIC); and Mahidol University under the National Research Universities Initiative.  
10  
11  
12  
13  
14  
15  
16  
17  
18  
19  
20  
21

## 22 References

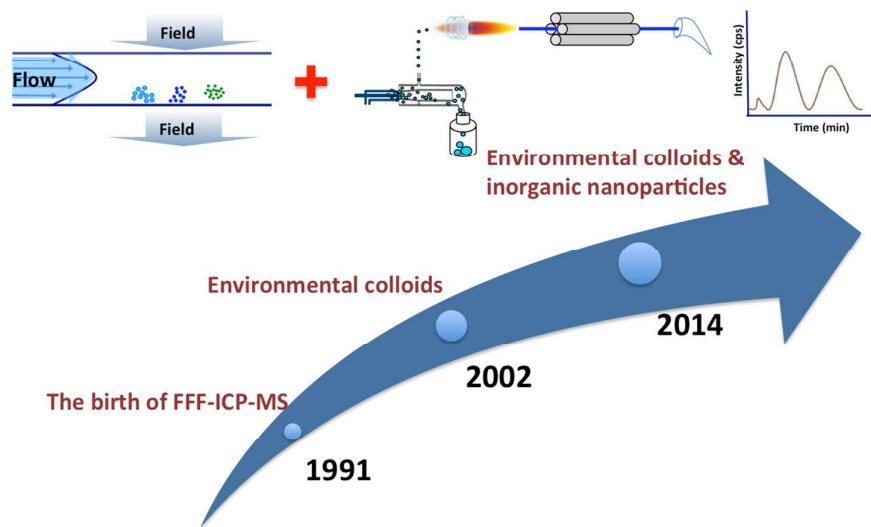
- 23 1. R. Beckett, *At. Spectrosc.*, 1991, **12**, 228-232.
- 24 2. M. Hassellöv, B. Lyvén, C. Haraldsson and W. Sirinawin, *Anal. Chem.*, 1999, **71**,  
25 3497-3502.
- 26 3. A. Siripinyanond and R. M. Barnes, *J. Anal. At. Spectrom.*, 1999, **14**, 1523-1526.
- 27 4. R. M. Barnes and A. Siripinyanond, in "Advances in Atomic Spectroscopy", ed. J.  
28 Sneddon, Elsevier, Amsterdam, Vol. 7 (2002), pp.179-235.
- 29 5. H. E. Taylor, J. R. Garbarino, D. M. Murphy and R. Beckett, *Anal. Chem.*, 1992,  
30 **64**, 2036-2041.
- 31 6. D. M. Murphy, J. R. Garbarino, H. E. Taylor, B. T. Hart and R. Beckett, *J.*  
32 *Chromatogr.*, 1993, **642**, 459-467.
- 33 7. S. Dubascoux, I. Le Hécho, M. Hassellöv, F. von der Kammer, M. Potin Gautier  
34 and G. Lespes, *J. Anal. At. Spectrom.*, 2010, **25**, 613-623.
- 35 8. K. Tiede, A. B. Boxall, S. P. Tear, J. Lewis, H. David and M. Hassellöv, *Food*  
36 *Addit. Contam. A*, 2008, **25**, 795-821.
- 37 9. M. S. Jiménez, M. T. Gómez, E. Bolea, F. Laborda and J. Castillo, *Int. J. Mass*  
38 *spectrom.*, 2011, **307**, 99-104.
- 39 10. P. Krystek, A. Ulrich, C. C. Garcia, S. Manohar and R. Ritsema, *J. Anal. At.*  
40 *Spectrom.*, 2011, **26**, 1701-1721.
- 41 11. P. S. Fedotov, N. G. Vanifatova, V. M. Shkinev and B. Y. Spivakov, *Anal*  
42 *Bioanal Chem*, 2011, **400**, 1787-1804.  
43  
44  
45  
46  
47  
48  
49  
50  
51  
52  
53  
54  
55  
56  
57  
58  
59  
60

12. M. Baalousha, B. Stolpe and J. R. Lead, *J. Chromatogr. A*, 2011, **1218**, 4078-4103.
13. G. Lespes and J. Gigault, *Anal. Chim. Acta*, 2011, **692**, 26-41.
14. C. Contado, G. Blo, C. Conato, F. Dondi and R. Beckett, *J. Environ. Monit.*, 2003, **5**, 845-851.
15. L. J. Gimbert, K. N. Andrew, P. M. Haygarth and P. J. Worsfold, *TrAC, Trends Anal. Chem.*, 2003, **22**, 615-633.
16. F. von der Kammer, S. Legros, T. Hofmann, E. H. Larsen and K. Loeschner, *TrAC, Trends Anal. Chem.*, 2011, **30**, 425-436.
17. E. Bolea, F. Laborda and J. R. Castillo, *Anal. Chim. Acta*, 2010, **661**, 206-214.
18. I. A. M. Worms, Z. Al-Gorani Szigeti, S. Dubascoux, G. Lespes, J. Traber, L. Sigg and V. I. Slaveykova, *Water Res.*, 2010, **44**, 340-350.
19. R. Krachler, R. F. Krachler, F. von der Kammer, A. Süphandag, F. Jirsa, S. Ayromlou, T. Hofmann and B. K. Keppler, *Sci. Total Environ.*, 2010, **408**, 2402-2408.
20. K. L. Plathe, F. von der Kammer, M. Hassellöv, J. Moore, M. Murayama, T. Hofmann and M. F. Hochella, *Envir. Chem.*, 2010, **7**, 82-93.
21. E. Neubauer, F. von der Kammer and T. Hofmann, *J. Chromatogr. A*, 2011, **1218**, 6763-6773.
22. C. Claveranne-Lamolère, J. Aupiais, G. Lespes, J. Frayret, E. Pili, F. Pointurier and M. Potin-Gautier, *Talanta*, 2011, **85**, 2504-2510.
23. S. R. Brittain, A. G. Cox, A. D. Tomos, E. Paterson, A. Siripinyanond and C. W. McLeod, *J. Environ. Monit.*, 2012, **14**, 782-790.
24. R. Henderson, N. Kabengi, N. Mantripragada, M. Cabrera, S. Hassan and A. Thompson, *Environ. Sci. Technol.*, 2012, **46**, 11727-11734.
25. T. Saito, Y. Suzuki and T. Mizuno, *Colloids Surf. A.*, 2013, **435**, 48-55.
26. B. Stolpe, L. Guo, A. M. Shiller and M. Hassellöv, *Mar. Chem.*, 2010, **118**, 119-128.
27. B. Stolpe, L. Guo, A. M. Shiller and G. R. Aiken, *Geochim. Cosmochim. Acta*, 2013, **105**, 221-239.
28. B. Stolpe, L. Guo and A. M. Shiller, *Geochim. Cosmochim. Acta*, 2013, **106**, 446-462.

- 1  
2  
3 29. A. J. Bednar, A. R. Poda, D. M. Mitrano, A. J. Kennedy, E. P. Gray, J. F.  
4 Ranville, C. A. Hayes, F. H. Crocker and J. A. Steevens, *Talanta*, 2013, **104**,  
5 140-148.  
6  
7  
8 30. M. E. Hoque, K. Khosravi, K. Newman and C. D. Metcalfe, *J. Chromatogr. A*,  
9 2012, **1233**, 109-115.  
10  
11 31. A. Ulrich, S. Losert, N. Bendixen, A. Al-Kattan, H. Hagedorfer, B. Nowack, C.  
12 Adlhart, J. Ebert, M. Lattuada and K. Hungerbühler, *J. Anal. At. Spectrom.*, 2012,  
13 **27**, 1120-1130.  
14  
15 32. E. Bolea, J. Jiménez-Lamana, F. Laborda and J. R. Castillo, *Anal. Bioanal. Chem.*,  
16 2011, **401**, 2723-2732.  
17  
18 33. A. R. Poda, A. J. Bednar, A. J. Kennedy, A. Harmon, M. Hull, D. M. Mitrano, J.  
19 F. Ranville and J. Steevens, *J. Chromatogr. A*, 2011, **1218**, 4219-4225.  
20  
21 34. J. G. Coleman, A. J. Kennedy, A. J. Bednar, J. F. Ranville, J. G. Laird, A. R.  
22 Harmon, C. A. Hayes, E. P. Gray, C. P. Higgins, G. Lotufo and J. A. Steevens,  
23 *Environ. Toxicol. Chem.*, 2013, **32**, 2069-2077.  
24  
25 35. A. R. Poda, A. J. Kennedy, M. F. Cuddy and A. J. Bednar, *J. Nanopart. Res.*,  
26 2013, **15**, 1673.  
27  
28 36. K. Loeschner, J. Navratilova, C. Købler, K. Mølhav, S. Wagner, F. von der  
29 Kammer and E. H. Larsen, *Anal. Bioanal. Chem.*, 2013, **405**, 8185-8195.  
30  
31 37. E. Bolea, J. Jimenez-Lamana, F. Laborda, I. Abad-Alvaro, C. Blade, L. Arola and  
32 J. R. Castillo, *Analyst*, 2014, **139**, 914-922.  
33  
34 38. B. Schmidt, K. Loeschner, N. Hadrup, A. Mortensen, J. J. Sloth, C. Bender Koch  
35 and E. H. Larsen, *Anal. Chem.*, 2011, **83**, 2461-2468.  
36  
37 39. E. P. Gray, T. A. Bruton, C. P. Higgins, R. U. Halden, P. Westerhoff and J. F.  
38 Ranville, *J. Anal. At. Spectrom.*, 2012, **27**, 1532-1539.  
39  
40 40. C. Contado and A. Pagnoni, *Anal. Chem.*, 2008, **80**, 7594-7608.  
41  
42 41. C. Contado and A. Pagnoni, *Anal. Methods*, 2010, **2**, 1112-1124.  
43  
44 42. A. Samontha, J. Shioatana and A. Siripinyanond, *Anal. Bioanal. Chem.*, 2011,  
45 **399**, 973-978.  
46  
47 43. V. Nischwitz and H. Goenaga-Infante, *J. Anal. At. Spectrom.*, 2012, **27**, 1084-  
48 1092.  
49  
50 44. I. López-Heras, Y. Madrid and C. Cámara, *Talanta*, 2014, **124**, 71-78.  
51  
52 45. H. E. Pace, E. K. Leshner and J. F. Ranville, *Environ. Toxicol. Chem.*, 2010, **29**,  
53 1338-1344.  
54  
55  
56  
57  
58  
59  
60

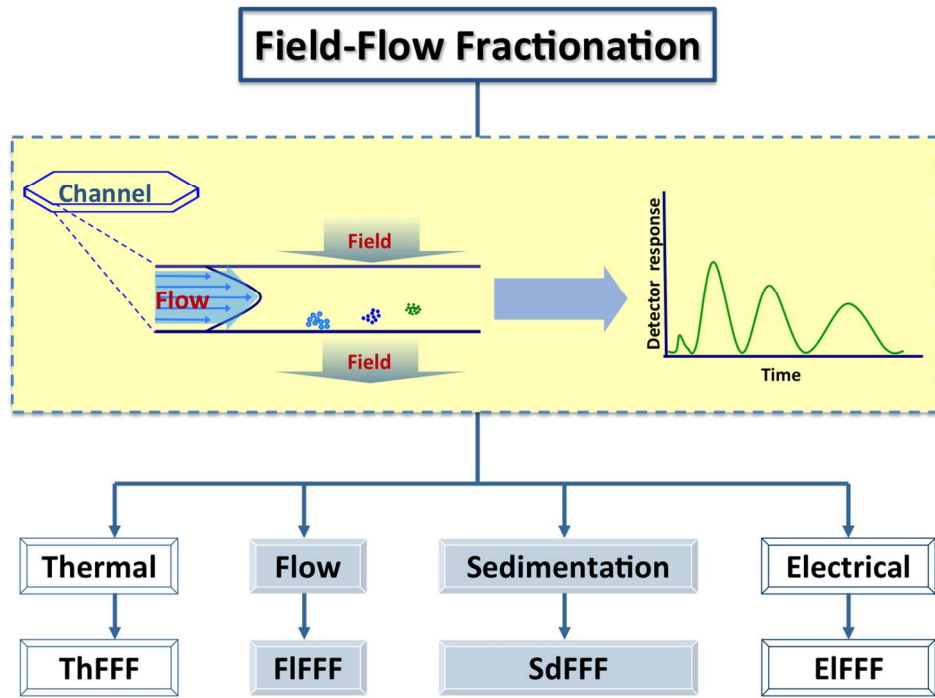
- 1
  - 2
  - 3
  - 4
  - 5
  - 6
  - 7
  - 8
  - 9
  - 10
  - 11
  - 12
  - 13
  - 14
  - 15
  - 16
  - 17
  - 18
  - 19
  - 20
  - 21
  - 22
  - 23
  - 24
  - 25
  - 26
  - 27
  - 28
  - 29
  - 30
  - 31
  - 32
  - 33
  - 34
  - 35
  - 36
  - 37
  - 38
  - 39
  - 40
  - 41
  - 42
  - 43
  - 44
  - 45
  - 46
  - 47
  - 48
  - 49
  - 50
  - 51
  - 52
  - 53
  - 54
  - 55
  - 56
  - 57
  - 58
  - 59
  - 60
46. W. Huang, D. Fernandez, A. Rudd, W. P. Johnson, D. Deubner, P. Sabey, J. Storrs and R. Larsen, *J. Chromatogr. A*, 2011, **1218**, 4149-4159.
47. P. M-M, W. Somchue, J. Shiowatana and A. Siripinyanond, *Food Research International*, 2014, **57**, 203-209.
48. J. Heroult, V. Nischwitz, D. Bartczak and H. Goenaga-Infante, *Anal. Bioanal. Chem.*, 2014, **406**, 3919-3927.
49. R. B. Reed, C. P. Higgins, P. Westerhoff, S. Tadjiki and J. F. Ranville, *J. Anal. At. Spectrom.*, 2012, **27**, 1093-1100.
50. D. M. Mitrano, A. Barber, A. Bednar, P. Westerhoff, C. P. Higgins and J. F. Ranville, *J. Anal. At. Spectrom.*, 2012, **27**, 1131-1142.
51. J. Szpunar, *TrAC, Trends Anal. Chem.*, 2000, **19**, 127-137.
52. J. Szpunar, *Analyst*, 2000, **125**, 963-988.
53. A. S. Al-Ammar, E. Reitznerová and R. M. Barnes, *Spectrochim. Acta B*, 1999, **54**, 1813-1820.
54. L. Rottmann and K. G. Heumann, *Fresenius J. Anal. Chem.*, 1994, **350**, 221-227.
55. L. Rottmann and K. G. Heumann, *Anal. Chem.*, 1994, **66**, 3709-3715.
56. J. Vogl and K. G. Heumann, *Fresenius J. Anal. Chem.*, 1997, **359**, 438-441.
57. J. Vogl and K. G. Heumann, *Anal. Chem.*, 1998, **70**, 2038-2043.
58. K. G. Heumann, S. M. Gallus, G. Raedlinger and J. Vogl, *Spectrochim. Acta B*, 1998, **53**, 273-287.
59. K. G. Heumann, *Anal. Bioanal. Chem.*, 2004, **378**, 318-329.
60. B. Meermann, A. L. Fabricius, L. Duester, F. Vanhaecke and T. Ternes, *J. Anal. At. Spectrom.*, 2014, **29**, 287-296.
61. J. Gigault, B. K. Gale, I. Le Hecho and G. Lespes, *Anal. Chem.*, 2011, **83**, 6565-6572.
62. W. Somchue, A. Siripinyanond and B. K. Gale, *Anal. Chem.*, 2012, **84**, 4993-4998.
63. S. Dubascoux, J. Heroult, I. Le Hécho, M. Potin-Gautier and G. Lespes, *Anal. Bioanal. Chem.*, 2008, **390**, 1805-1813.
64. M. Abu-Farha, F. Elisma, H. Zhou, R. Tian, H. Zhou, M. S. Asmer and D. Figeys, *Anal. Chem.*, 2009, **81**, 4585-4599.
65. Z. Ning, H. Zhou, F. Wang, M. Abu-Farha and D. Figeys, *Anal. Chem.*, 2011, **83**, 4407-4426.

- 1  
2  
3  
4  
5  
6  
7  
8  
9  
10  
11  
12  
13  
14  
15  
16  
17  
18  
19  
20  
21  
22  
23  
24  
25  
26  
27  
28  
29  
30  
31  
32  
33  
34  
35  
36  
37  
38  
39  
40  
41  
42  
43  
44  
45  
46  
47  
48  
49  
50  
51  
52  
53  
54  
55  
56  
57  
58  
59  
60
- Figure 1 FFF principle and sub-techniques.  
In FFF, separations are achieved within a flat open channel with a rectangular cross-section and triangular end pieces where the sample and carrier liquid enter and leave. The essence of FFF is to apply a force perpendicular to the channel flow stream, which is a parabolic flow profile. This force drives macromolecules or particles toward an accumulation wall where they encounter slow-moving laminar fluid streamlines. Fractionation is achieved by the balance between the applied field force pushing the sample particles toward the accumulation wall and the diffusivity of sample particles acting against the field force. Smaller species diffuse away from the accumulation wall into the carrier stream faster than larger species. Thus, various size sample components are driven into different average positions axially and laterally in the channel flow. Consequently, each sample component leaves the channel at a different time related to its diffusion coefficient and thus molecular weight. These primary driving forces can be generated by a number of fields or gradients, resulting in numerous FFF sub-techniques that are generally applicable to different materials.
- Figure 2 Publication trend on “FFF” with “ICP” since 1992.
- Figure 3 Publications on “FFF” with “ICP” since 1992 as classified by country.
- Figure 4 Publications on “FFF” with “ICP” since 1992 as classified by the institution.

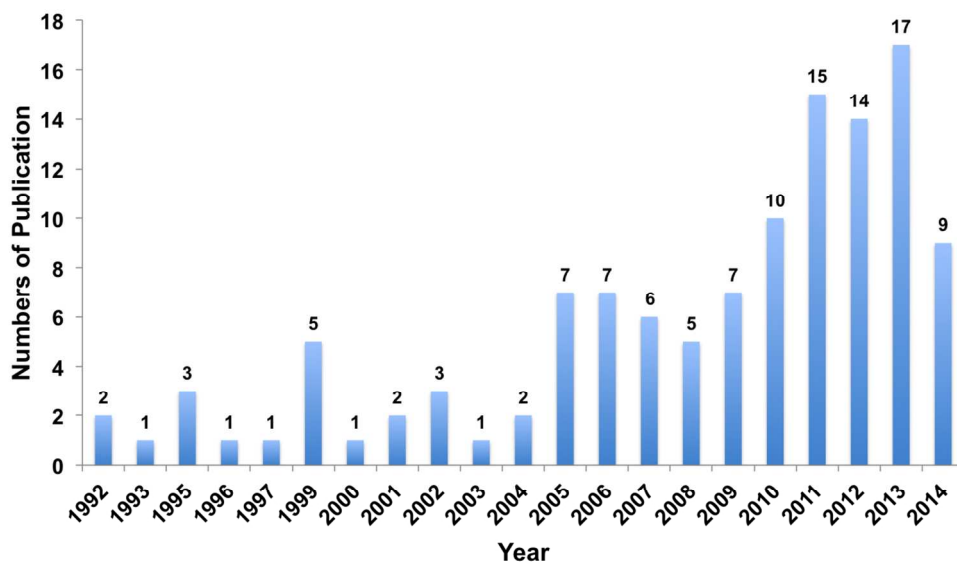


Historical background, recent applications, and future trends of field-flow fractionation-inductively coupled plasma mass spectrometry

1  
2  
3  
4  
5  
6  
7  
8  
9  
10  
11  
12  
13  
14  
15  
16  
17  
18  
19  
20  
21  
22  
23  
24  
25  
26  
27  
28  
29  
30  
31  
32  
33  
34  
35  
36  
37  
38  
39  
40  
41  
42  
43  
44  
45  
46  
47  
48  
49  
50  
51  
52  
53  
54  
55  
56  
57  
58  
59  
60

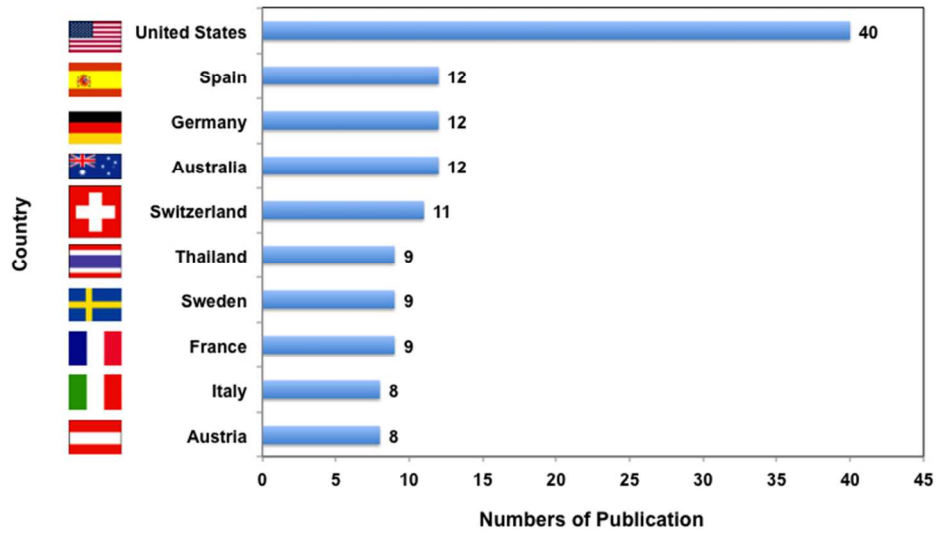


508x381mm (72 x 72 DPI)



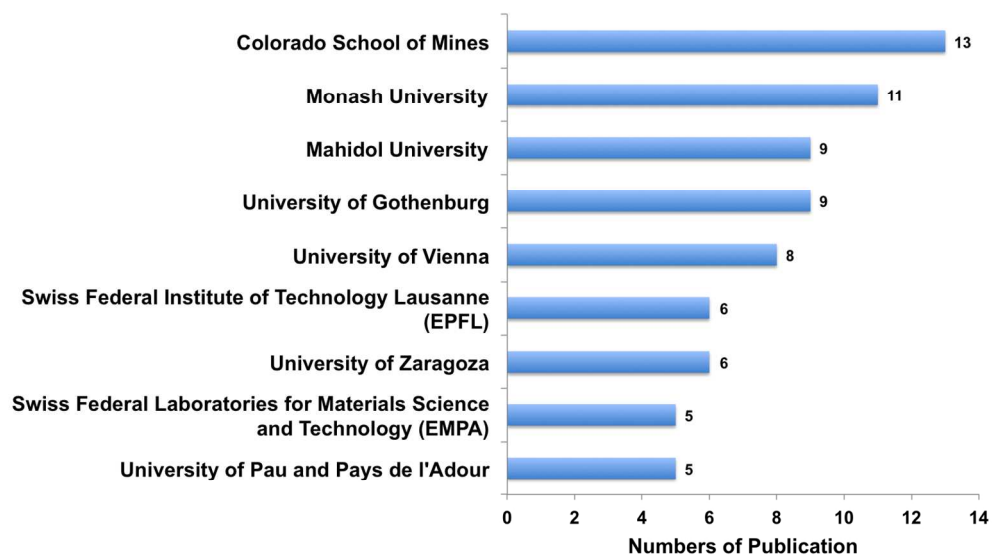
230x135mm (150 x 150 DPI)

1  
2  
3  
4  
5  
6  
7  
8  
9  
10  
11  
12  
13  
14  
15  
16  
17  
18  
19  
20  
21  
22  
23  
24  
25  
26  
27  
28  
29  
30  
31  
32  
33  
34  
35  
36  
37  
38  
39  
40  
41  
42  
43  
44  
45  
46  
47  
48  
49  
50  
51  
52  
53  
54  
55  
56  
57  
58  
59  
60



282x159mm (72 x 72 DPI)

1  
2  
3  
4  
5  
6  
7  
8  
9  
10  
11  
12  
13  
14  
15  
16  
17  
18  
19  
20  
21  
22  
23  
24  
25  
26  
27  
28  
29  
30  
31  
32  
33  
34  
35  
36  
37  
38  
39  
40  
41  
42  
43  
44  
45  
46  
47  
48  
49  
50  
51  
52  
53  
54  
55  
56  
57  
58  
59  
60



275x159mm (150 x 150 DPI)

1  
2  
3  
4  
5  
6  
7  
8  
9  
10  
11  
12  
13  
14  
15  
16  
17  
18  
19  
20  
21  
22  
23  
24  
25  
26  
27  
28  
29  
30  
31  
32  
33  
34  
35  
36  
37  
38  
39  
40  
41  
42  
43  
44  
45  
46  
47  
48  
49  
50  
51  
52  
53  
54  
55  
56  
57  
58  
59  
60